Jurnal Teknologi

Full paper

Quantitative Hazard Analysis for Landslides in Hulu Kelang area, Malaysia

Nader Saadatkhah[a], Azman Kassim[a,*], Lee Min Lee[b], Gambo Haruna Yunusa[a]

[a]*Department of Geotechnics and Transportation, Faculty of Civil Engineering, Universiti Teknologi Malaysia, 81310 UTM Johor Bahru, Johor Malaysia*
[b]*Faculty of Engineering and Science, Universiti Tunku Abdul Rahman, 53300 Kuala Lumpur, Malaysia*

*Corresponding author: azmankassim@utm.my

Article history

Received: 18 May 2014
Received in revised form:
16 November 2014
Accepted: 1 February 2015

Graphical abstract

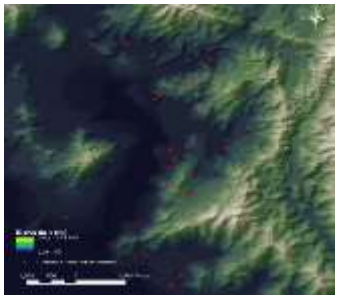

Abstract

Hulu Kelang is a region in Malaysia which is very susceptible to landslides. From 1990 to 2011, a total of 28 major landslide events had been reported in this area. This paper evaluates and compares the probability-frequency ratio (FR), statistical index (Wi), and weighting factor (Wf), used for assessing landslide susceptibility in the study area. Eleven landslide influencing factors were considered in the analyses. These factors included lithology, land cover, curvature, slope inclination, slope aspect, drainage density, elevation, distance to lake and stream, distance to road and trenches and two indices (the stream power index (SPI) and the topographic wetness index (TWI)) found in the area. The accuracy of the maps produced from the three models was verified using a receiver operating characteristics (ROC). The verification results indicated that the probability-frequency ratio (FR) model which was developed quantitatively based on probabilistic analysis of spatial distribution of historical landslide events was capable of producing a more reliable landslide susceptibility map in this study area compared to its other counterparts. About 89% of the landslide locations have been predicted accurately by using the FR map.

Keywords: Landslide susceptibility, probability-frequency ratio, bivariate approach

1.0 INTRODUCTION

Landslide susceptibility is considered as the susceptibility of the terrain to defined slope failures. A landslide hazard map explains regions probably to have landslides in the future. Landslide losses in all parts of the world are likely to increase continuously, as growing population, combined with the need to protect natural and agricultural areas, presses human developments ever closer to unstable slopes. The only way to reduce such losses is to develop a better understanding of landslide processes and more reliable techniques of predicting their potential effects and designing remedial or protective measures. Hence, the identification of landslide-prone regions is essential for carrying out quicker and safer mitigation programs, as well as future planning of the area.

Nilsen et al. (1979) developed the earliest methods used to assess the risk of landslides by laying qualitative morphological and geological slope-characteristics over landslide inventories. State of the art research pertaining to landslide susceptibility mapping has witnessed the development of sophisticated assessment techniques that have included inventory, bivariate, multivariate, probabilistic frequency ratio, logistics regression, fuzzy logic, such as the analytical hierarchy process (AHP), probabilistic frequency and artificial neural network analysis (Van-Westen, 1997; Dai et al., 2001; Lee and Min, 2001; Ercanoglu and Gokceoglu, 2004; Lee, 2005; Pradhan et al., 2006; Dahal et al., 2008; Sarkar et al., 2008, Sarkar and Anbalagan 2008; Dwikorita et al., 2011).

Quantitative models use a numerical assessment of the relationship between slope instability and other controlling factors. Two examples of a quantitative method are deterministic and statistical methods, which were frequently used in previous landslide susceptibility studies (Ercanoglu and Gokceoglu, 2002; Suzen and Doyuran, 2004; Ercanoglu and Gokceoglu, 2004; Yesilnacar and Topal, 2005; Kanungo et al. 2006; García-Rodríguez et al. 2008; Nefeslioglu et al. 2008; Nandi and Shakoor, 2009; Dongyeob et al., 2010; Pradhan, 2012 etc.). Deterministic approaches are mainly based on factor of safety (FOS) computation (Refice and Capolongo 2002; Zhou et al. 2003), while statistic methods focus on historical correlations between landslide-controlling parameters and the distribution of landslide events.

The goal of this study was to compare and evaluate quantitative methods including a probabilistic frequency ratio (FR) model, a statistical index (Wi) and weighting factor (Wf) techniques for their ability to assess the probabilistic frequency landslide susceptibility of a case study. The probabilistic frequency ratio draws on data regarding the distribution and effectiveness of factors that causes landslides to determine the correlation between regions and these factors (Lee, 2005). Bivariate methods combine factor maps with landslide

distribution maps. Weighted values are found for each factor or class of factors (Oztekin and Topal, 2005; Conoscenti et al., 2008; Nandi and Shakoor, 2009). Finally, the landslide susceptibility maps created as a result of this process are subjected to a comprehensive validation process. The models are validated using either data for landslides that was used to create the map or independent landslide information can be used (Chung and Fabbri, 2003; Guzzetti et al., 2005, 2006). This study used landslide data that was divided into two groups, a modeling group (70% of the total landslide events) and a prediction group (30% of the total landslide events). The modeling group was used as a training set for the development of landslide susceptibility maps that built on the three models discussed earlier (probabilistic frequency ratio, Wi, and Wf models) while the prediction group was used for verification purposes.

1.1 Background Of The Study Area

Hulu Kelang is known as one of the most landslide susceptible areas in Malaysia. From 1990 to 2011, a total of 28 major landslide events had been reported in this area (Lee et al., 2013). Hulu Kelang is in Kuala Lumpur, the capital city of Malaysia and is located between latitude 101° 44′ 13" and 101°47′ 51"N and Longitude 3° 09′ 25" and 3° 13′ 45" E as presented in Figure 1.

Soil investigations from previous studies revealed that the area rests on coarse-grained granite (Ali, 2000). Weathering of the granite produced sandy clay residual soil of approximately 15 to 30 m thick at areas of high elevation. The residual soil layer becomes thinner on the mid-course of slopes (Lee et al., 2009), followed by exposed granite at the low elevation areas. Landslide slip planes commonly develop in residual soil layers.

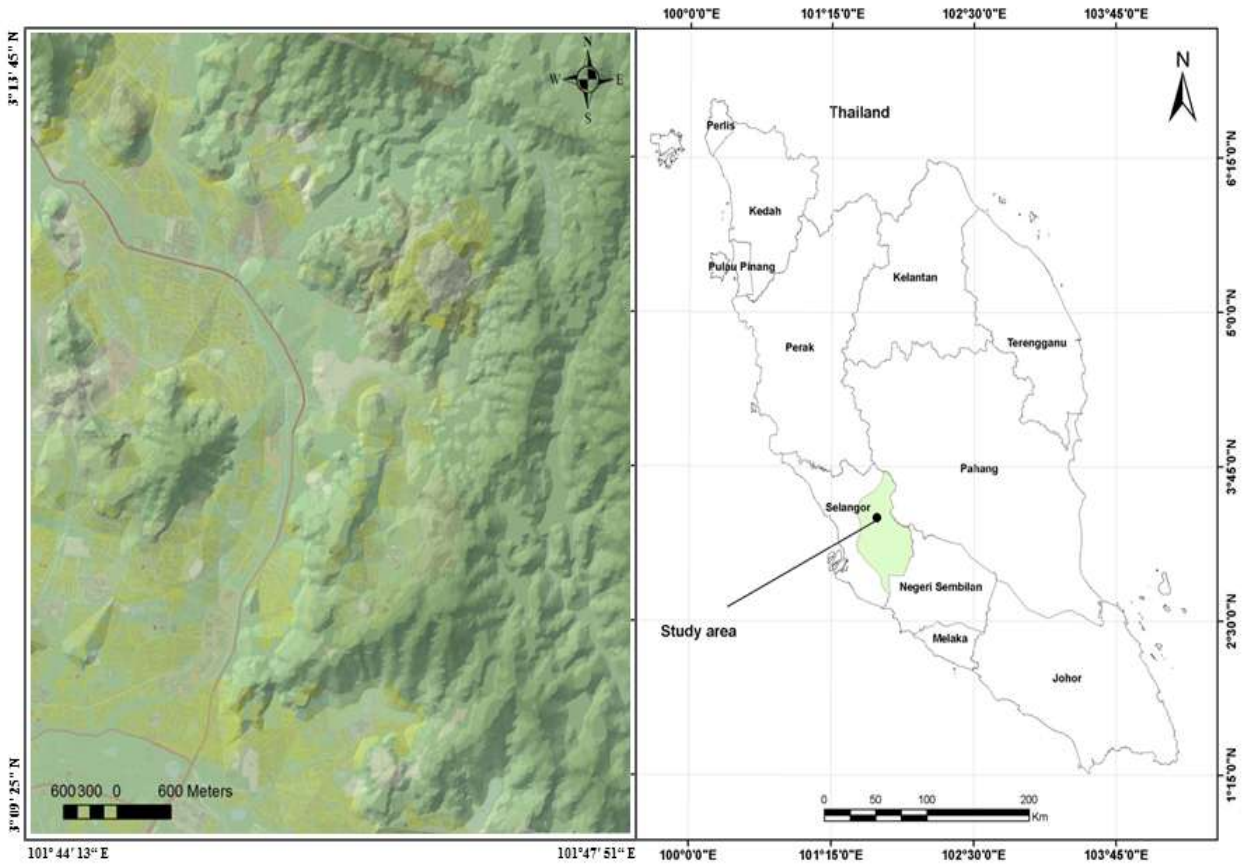

Figure 1 Location of Hulu Kelang area, Serdang, Malaysia (Saadatkhah et al. 2014)

2.0 MATERIAL AND METHODS

2.1 Layers Of Thematic Data

This study began with data from past landslides found in previous reports, it is essential to document the distribution of landslides in an area, to investigate the extent, sample and types of landslide, and to determine landslide susceptibility, hazard, and vulnerability. According to the data sources from the Ampang Jaya Municipal Council (MPAJ) and the Slope Engineering Branch of Public Works Department Malaysia (PWD), a total of 28 major historical landslide events have been reported in the Hulu Kelang area from 1990 to 2011 as shown in Figure 2.

The lithological settings in the study area can generally be classified into three main types, namely granite, phyllite and schist, and limestone. The analysis of landslide distribution and lithological units performed in this area revealed that 72.73% of the historical landslide events in Hulu Kelang occurred on highly or completely weathered granitic rock formation, while the remaining 27.27% of the landslides were located on phyllite and schist rock as presented in Table 1.

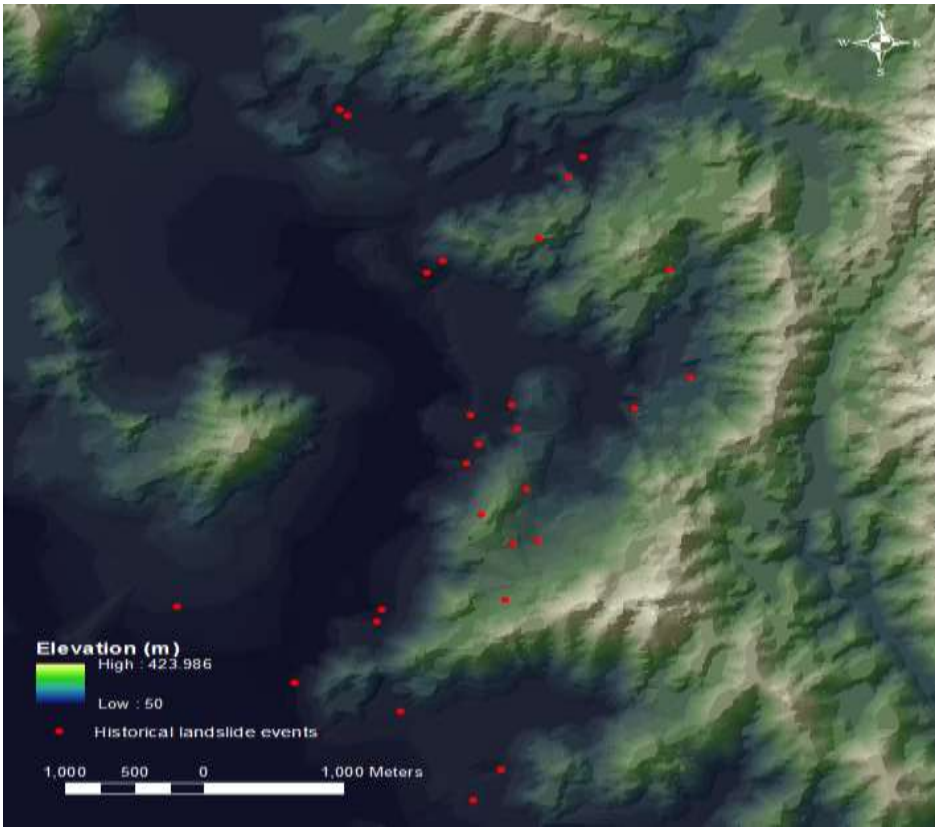

Figure 2 Landslide Inventory Map of Hulu Kelang Area

Land covers could act as a buffer to limit rainwater infiltration into soil slopes by evapo-transpiration from the canopies (interception loss) and, to a lesser extent, absorbed by plants (Rutter et al., 1971, 1975). Under the classification system, eight types of land covers were identified, i.e. primary forest, secondary jungle, rubber, sundry tree cultivation, grassland, cleared land, developed area, and lake. Historical slope failures were mainly scattered on the rubber and grassland areas. These land covers with no canopy allow for more rainfall infiltration, which increases soil pore-water pressure and increases the potential for landslides (Table 1).

Slope inclination is one of the factors used to controls areal hydraulic continuity, and consequently factor of safety of slopes. In this study, six categories of slopes were used (0-10º, 10-20 º, 20-30 º, 20-40 º, 40-50° and 50-90 º). Based on the distributions of the historical landslide events, it was found that 98.8% of the landslides occurred on slopes between 0 and 40° (Table 1).

Table 1 Frequency ratio, Wi and Wf values of the data layers

Factor	Class	% of total area	% of landslide area	Frequency ratio	Wi*	Wf**
Lithology	Granite	54.08	44.08	1.345	0.296	46.52
	Phyllite-schist	42.51	16.53	0.642	-0.444	
	Limestone	3.41	0.00	0.000	0	
Landcover	Primary forest	31.61	7.35	0.383	-0.958	100
	Secondary forest	1.88	2.20	1.934	0.661	
	Rubber	14.29	21.67	2.502	0.917	
	Sundry tree cultivation	1	0.00	0.000	0	
	Grassland	2.87	3.67	2.112	0.748	
	Cleared land	4.64	2.57	0.914	-0.089	
	Developed area	43.25	23.14	0.883	-0.125	
	Lake	0.47	0.00	0.000	0	
Slope Inclination	0-10	56.69	32.32	0.941	-0.061	41.89

	10-20	15.16	15.43	1.679	0.518	
	20-30	22.01	9.92	0.743	-0.296	
	30-40	5.54	2.20	0.656	-0.421	
	40-50	0.49	0.73	2.474	0	
	50-90	0.11	0.00	0.000	0	
Slope Aspect	North	5.77	6.61	1.891	0	91.20
	Northeast	5.08	2.57	0.835	-0.181	
	East	7.5	7.35	1.616	0.480	
	Southeast	8.75	0.37	0.069	0	
	South	8.08	7.71	1.575	0.455	
	Southwest	8.75	3.67	0.693	-0.367	
	West	10.77	1.47	0.225	0	
	Northwest	7.93	8.45	1.758	0.564	
	Flat	37.37	22.41	0.989	-0.011	
Plan Curvature	Concave	34.87	23.88	1.130	0.122	51.72
	Flat	30.89	17.63	0.942	-0.060	
	Convex	34.24	19.10	0.920	-0.083	
Elevation	0-100	48.24	34.89	1.194	0.177	71.52
	100-200	31.92	25.71	1.329	0.284	
	200-300	17.99	0.00	0.000	0	
	300-425	1.85	0.00	0.000	0	
Distance to the roads and trenches	0-25	10.13	11.75	1.915	0.650	68.01
	25-50	13.22	19.83	2.476	0.907	
	50-75	7.22	1.47	0.336	-1.091	
	75-100	5.82	2.94	0.833	-0.182	
	100-125	5.04	6.61	2.165	0.772	
	125<	58.57	18.00	0.507	-0.679	
Distance to lake and streams	0-25	12.29	6.61	0.888	-0.119	0.01
	25-50	22.11	9.92	0.740	-0.301	
	50-75	12.51	8.45	1.114	0	
	75-100	8.74	3.31	0.624	-0.471	
	100-150	10.96	2.20	0.332	-1.103	
	150-200	5.86	2.57	0.724	-0.323	
	200-250	5.26	7.35	2.304	0.836	
	250<	22.26	16.53	1.225	0.203	
Drainage density	0-0.0025	44.22	11.75	0.439	-0.824	88.86
	0.0025-0.005	8.69	0.00	0.000	0	
	0.005-0.0075	8.88	2.94	0.546	-0.605	
	0.0075-0.01	14.17	19.10	2.224	0.799	
	0.01-0.0125	10.89	15.06	2.282	0.825	
	0.0125_0.015	9.74	11.75	1.991	0.689	
	0.015-0.03	0.62	0.00	0.000	0	
	0.03-0.135	2.78	0.00	0.000	0	
Topographic wetness index (TWI)	6-9.32	0.00	0.00	0.858	0	93.19
	9.32-11.04	0.62	0.00	0.000	0	
	11.04-12.76	7.58	4.85	0.000	-0.447	
	12.76-14.48	11.61	24.24	0.640	0.737	
	14.48-16.2	3.09	6.06	2.089	0.674	
	16.2-17.9	0.59	0.61	1.962	0.025	
	17.9-19.3	0.59	0.00	1.025	0	
Stream power index (SPI)	6-8.74	1.15	0.61	0.000	-0.642	87.63
	8.74-10.44	0.94	0.00	0.858	0	
	10.44-12.15	3.08	6.06	0.526	0.677	
	12.15-13.85	11.88	13.94	0.000	0.160	
	13.85-15.56	7.53	14.55	1.968	0.658	
	15.56-16.6	0.51	0.00	1.173	0	

Note: *Wi was calculated from equation 2
**Wf was calculated from equation 3

Slope aspect as another factors used, influences intensity of rainfalls received on a sloping surface and weathering process in a soil slope (Cevik and Topal, 2003; Lee, 2005; Galli et al., 2008). Nine different regions were investigated in the present study: flat area (−1°), north (337.5°–22.5°), northeast (22.5°–67.5°), east (67.5°–112.5°), southeast (112.5°–157.5°), south (157.5°–202.5°), southwest (202.5°–247.5°), west (247.5°–292.5°), and northwest (292.5°–337.5°). Slopes facing the same direction as the monsoons (northeast and southwest) are more prone to landslides. Observations from the landslide inventory map revealed that

about 48.5% of the landslides occurred on the slopes inclined to these directions (Table 1).

The term curvature as one of the factors used in the study area defines the morphology of topography. Curved land normally increases the moisture content of soil, keeps the soil saturated, and consequently increases the susceptibility of slopes to erosion and landslides. In this study, three zones were identified based on their plan curvatures: positive curvature (convex), negative curvature (concave), and zero curvature representing flat surface. The analysis of landslide distribution density showed that 40% of the landslides located in the concave zone, while 31% of the landslides occurred in the convex zone (Table 1).

The elevation factor influences the surface of the terrain and other topographical characteristics such as profile curvatures, the angle and aspect of a slope, and the determination of catchment areas and planning concerns(Wilson and Gallant, 2000; Gruber and Peckham, 2008) in the study area. The area investigated in this study ranged in elevation from 0 to 425m above sea level. Most of the landslide distribution densities occurred at 0–100 m (57.6%) and 100-200 m (42.4%) (Table 1).

Distance to road construction activities such as soil excavation, imposing of surcharge load, cut slope, embankment construction, and removal of vegetation cover may cause failures to the slopes which are otherwise stable. Six regions were identified in this study based on their distances from roadways (0-25 m, 25-50 m, 50-75 m, 75-100 m, 100-125 m, and less than 125 m). About 86% of past landslides occurred 0 –50 m from a roadway (Table 1).

Several studies have shown that susceptibility to landslides could be affected by preferential flows in soil (Tsukamoto et al., 1982; Sidle et al., 2000, 2006; Uchida et al., 2002) and rock masses (Montgomery et al., 1997; Uchida et al., 2002 ; Sidle and Chigira, 2004). In this area, distance to stream as one of the factors used represented at eight buffer zones (0–25 m, 25–50 m, 50–75 m, 75–100 m, 100-150 m, 150-200 m, 200-250 m, and less than 250 m) based on their proximity to where are identified as shown in Table 1. Most of the historical landslides were located between 0 and 75 m from a stream.

Drainage density is defined as the proportion of the total length of the water flow to the total area of the drainage basin. Drainage networks also as one of factor used in this study were extracted directly from the digital elevation map (DEM). Eight drainage buffer zones were produced to define the extent of slope instability caused by streams. These drainage buffer zones were: Zone A (0-0.0025m^{-1}), Zone B (0.0025-0.005m^{-1}), Zone C (0.005-0.0075m^{-1}), Zone D (0.0075-0.01m^{-1}), Zone E (0.01-0.0125m^{-1}), Zone F (0.0125-0.015m^{-1}), Zone G (0.015-0.03m^{-1}), and Zone H (0.03-0.135m^{-1}). The drainage density analyses showed that all the historical landslides occurred within the density range of 0–0.015 m^{-1} (Table 1).

The Compound Topographical Index is also known as the Topographic Moisture Index and Saturation Conditions or the Topographic Wetness Index (TWI) that used in this study. The TWI is a ratio of contributing catchment area to slope inclination (Wilson and Gallant, 2000). The study area was divided into eight different classes of TWI ranging from 0 to 19.3. Table 1 shows that 35.76% of the historical landslides occurred within the TWI range of 11.04-17.9.

The Stream Power Index (SPI) is a way of measuring the power of surface water to erode surfaces based on the hypotheses that discharge (q) is proportional to the specific catchment area (As). The SPI value is governed by two parameters: viscosity of the land slope and steepness of the terrain. Seven SPI classes were used in this study and they ranged from 0 to 16.6. The SPI analysis showed that 57% of the historical landslides occurred within the SPI range of 10.44–15.56 (Table 1).

3.0 ANALYSIS OF LANDSLIDE SUSCEPTIBILITY

In this study, an analysis of the susceptibility to landslides was carried out using the probabilistic frequency ratio, and bivariate (Wi and Wf) models. Prior to the analyses, the factors affecting landslides in Hulu Kelang area were identified. In this study, the DEM was derived using photogrammetric techniques. A series of aerial photographs from 1966 to 2003 were provided by department of surveying and mapping Malaysia (JUPEM). In particular, aerial photographs from the 2003 flight were sufficient to cover the study areas. The cloud of photographic points extracted from aerial photographs data was therefore imported into a GIS environment. In addition to the points obtained using the photogrammetric analysis, the contour lines of the Regional Topographical Map at a 1: 10000 scale is extracted in standard topographic Ampang and Kampung Kelang Gates Baharu maps. The pixel dimensions used was 30×30m pixel for the landslide and factor maps. Landslide regions were defined using the landslide inventory map and satellite images.

3.1 Probabilistic Frequency Ratio Model

A probabilistic frequency ratio model used GIS techniques to quantitatively construct a landslide susceptibility map. The probabilistic frequency ratio method is based on the distribution of landslides and the parameters related to landslides so that the correlation between the location of the landslide and the parameters for the area can be represented (Pradhan et al., 2010). The first step was to calculate the frequency ratio for each parameter based on its relationship to landslides, as shown in Table 1. Next, the frequency ratio for the sub-criteria of each parameter was calculated. These ratios were used to find the landslide susceptibility index (LSI) (refer to Eq. 1) (Lee and Pradhan, 2007).

$$LSI = Fr1 + Fr2 + Fr3 + \ldots + Frn \quad [1]$$

Where, Fr is the rating for each parameter. According to the probabilistic frequency ratio method, an average LSI has a value of unity. A value of > 1 indicates that there is a strong relationship between the landslide and the parameter being investigated (Akgun et al., 2007).

3 2 Bivariate Statistics Method

This study used a statistical bivariate model based on Wi (Van-Westen, 1997) and Wf approaches, which are widely considered to be a simple and quantitative method of susceptibility mapping (Cevik and Topal, 2003; Lan et al.,

2004; Wang and Sassa, 2005; Thiery et al., 2007; Dahal et al., 2008), were used to compute the distribution of landslides for each factor class. These density values can be standardized by correlating them to the overall density in an area (Oztekin and Topal, 2005). In this study, the Wi for each class was computed using the formula proposed by vanWesten (1997):

$$Wi = In\frac{Densclass}{Densmap} = In\frac{\frac{Npix\,(Si)}{Npix(Ni)}}{\frac{SNpix(Si)}{SNpix(Ni)}} \quad [2]$$

Where, *Wi* is the weight given to a determined class of parameter. *Densclass* refers to the landslide density within the class of parameter and the *Densmap* is the landslide density for the whole map. *Npix(Si)* is the number of pixels that contain a determined parameter class of landslide, *Npix(Ni)* is the total number of pixels for a determined parameter class, *SNpix(Si)* is the total number of pixels in all the landslides, and *SNpix(Ni)* it the total number of all pixels.

Table 1 shows the Wi value of each computed attribute. All the layers were laid on top of one another to create a susceptibility map. The Wi susceptibility map was separated into equal classes labeled very low, low, moderate, high, very high, and critical susceptibility. However, these maps indicate that each factor map had an equal effect on landslides, which is not an accurate reflection of what really happens (Oztekin and Topal, 2005). To resolve this issue, a Wf was produced for each factor shown on a map. The first step in this process is to define the Wi value of each pixel using the Wi method. In the next step, the values for all the pixels within the landslide zones for each layer were added together. The results were stretched using the maximum and minimum for all layers (Cevik and Topal, 2003).The weighting factors that ranged from 1 to 100 for each layer were defined using the formula shown below:

$$Wf = \frac{(TWi_{value})-(MinTWi_{value})}{(MaxTWi_{value})-(MinTWi_{value})} \text{ x } 100 \quad [3]$$

Where, *Wf* is the calculated weighting factor for each layer and TWi_{value} is the total weighting index value of the cells in the landslide bodies for each layer. The minimum total weighting index value in selected layers is represented using $MinTWi_{value}$ and the Maximum total weighting index value within selected layers is calculated using $MaxTWi_{value}$.
In this analysis, the Wf value was multiplied by the Wi value. All the factors shown on the map were added together to determine final landslide susceptibility.

4.0 RESULTS AND DISCUSSION

The landslide susceptibility maps produced from the three prescribed approaches, i.e. probabilistic frequency ratio, statistical index (Wi), and weighting factor (Wf) models yielded six susceptibility classes, namely very low (the lowest susceptibility), low, moderate, high, very high, and critical (the highest class) susceptibility.

4.1 Prediction of Landslide Susceptibility Maps

Different weight factors and ratios were used to evaluate the spatial relationship between landslides and landslide conditioning factors. The frequency ratio for probabilistic frequency ratio model, Wi and Wf values for statistical index and weighting factor models are tabulated in Tables 2, 3, and 4, respectively. In general, these assigned weight factor / ratio / index showed good agreement with the historical landslide data and fundamental theories of slope stability. Based on the weight factor / ratio / index assigned for each landslide influencing factors, the landslide susceptibility maps produced using probabilistic frequency ratio, Wi, and Wf models are presented in Figures 3 to 5, respectively.

Table 2 Summary of FR model results in landslide simulations

FR	Landslide site (a)	% of landslide site (c) =a/b	% of predicted area (d)	LR_{class} (e) =c/d	% of LR_{class} = e/f
Very low	0	0	4.34	0.00	0.00
Low	28	11	43.22	0.26	0.72
Moderate	99	40	37.35	1.07	2.93
High	83	33	12.89	2.60	7.11
Very high	27	11	2.02	5.38	14.75
Critical	12	5	0.18	27.19	74.51
Sum	249 (b)	100.000	100.00	36.49(f)	100.00

Table 3 Summary of Wi model results in landslide simulations

Wi	Landslide site (a)	% of landslide site (c) =a/b	% of predicted area (d)	LR_{class} (e) =c/d	% of LR_{class} = e/f
Very low	4	2	7.30	0.22	1.16
Low	82	33	56.83	0.58	3.05
Moderate	80	32	30.77	1.05	5.50
High	75	30	4.67	6.47	33.96
Very high	8	3	0.30	10.73	56.31
Critical	0	0	0.13	0	0
Sum	249 (b)	100.000	100.00	19.06 (f)	100.00

Table 4 Summary of Wf model results in landslide simulations

Wf	Landslide site (a)	% of landslide site (c) =a/b	% of predicted area (d)	LR_{class} (e) =c/d	% of LR_{class} = e/f
Very low	11	4.42	21	0.21	1.67
Low	103	41.37	55.27	0.75	5.94
Moderate	83	33.33	21.32	1.56	12.41
High	52	20.88	2.07	10.08	80
Very high	0	0	0.23	0	0
Critical	0	0	0.10	0	0
Sum	249 (b)	100	100	12.6(f)	100

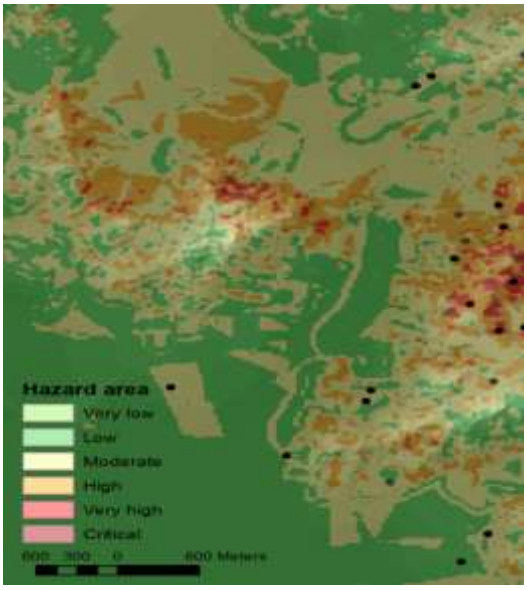

Figure 3 Landslide susceptibility map produced from probabilistic-frequency ratio (FR) model

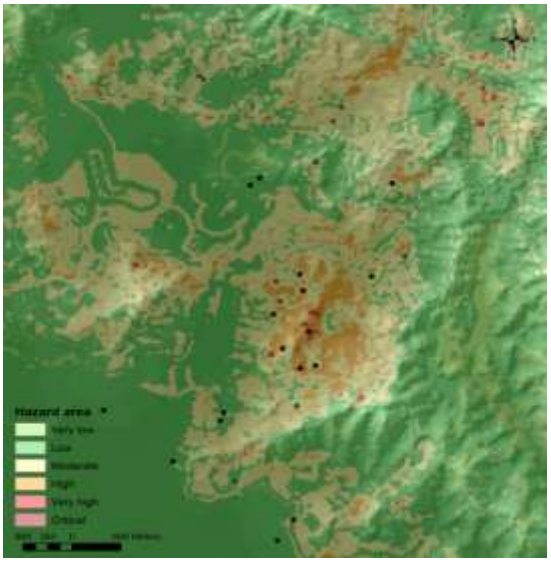

Figure 4 Landslide susceptibility map produced from statistical index (Wi) model

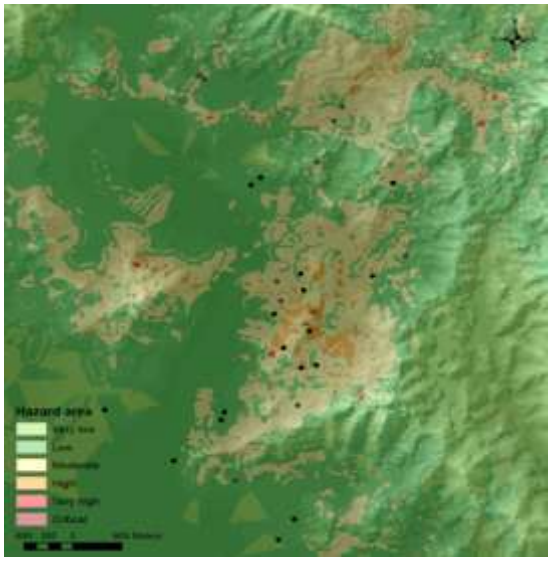

Figure 5 Landslide susceptibility map produced from weighting factor (Wf) model

One main objective of this study was to evaluate the spatial predictability of landslide events in Hulu Kelang area, using the landslide susceptibility maps produced from probabilistic frequency ratio, Wi, and Wf models. The success of landslide prediction model has been typically evaluated by comparing locations of measured landslides with the predicted results. Therefore, the landslide ratio of each predicted hazard class (landslide ratio for each predicted hazard class) was employed for evaluating the performance of the landslide model. Landslide ratio for each predicted hazard class (LR_{class}) was based on the ratio of landslide sites contained in each hazard class, in relation to the total number of actual landslide sites, according to the predicted percentage of area in each class of hazard category.

$$LR_{class} = \frac{\%\ of\ contained\ landslide\ sites\ in\ each\ class\ of\ hazard}{\%\ of\ predicted\ landslide\ areas\ in\ each\ class\ of\ hazard} \quad [4]$$

Note that in the numerator, the number of landslide sites, instead of the number of landslide cells, is used. The performance value derived from LR_{class} enables consideration of predicted stable areas as well as predicted

unstable areas, and thus substantially reduces the over-prediction of landslide potential. Unlike the numerator, the number of predicted and total cells is used in denominator. The numerator, also, is the same as the SR (Success Ratio) index. Tables 2, 3, and 4 show that 15.09%, 5.1%, and 2.4% of the area were classified as unstable (Hazardous area ≥ High), while that 49%, 33%, and 20.88% of the actual landslides were correctly localized within this predicted unstable areas, respectively. FR model represented the LR_{class} ≥ High about 35.17 by calculating the % of LR_{class} equal to 96.37% (Figure 6a). The % of LR_{class} ≥ High of Wi model presented about 90.27% by calculating the LR_{class} equal to 17.2 (Figure 6b). And Wf model represented the LR_{class} ≥ High about 10.08 by calculating the % of LR_{class} equal to 80% (Figure 6c). If a landslide happens, then predicted unstable area (Hazardous area ≥ High) has 96.37% chance of including the landslide using Fr model and have 90.27% and 80% chances using Wi, Wf models, respectively. These results indicated that the frequency ratio model was the landslide susceptibility mapping method preferred for use in this study as the resultant map contained a relatively low percentage of active landslide zones in the very low and low susceptibility classes, and a high percentage of active landslide zones in the high, very high and critical susceptibility zones.

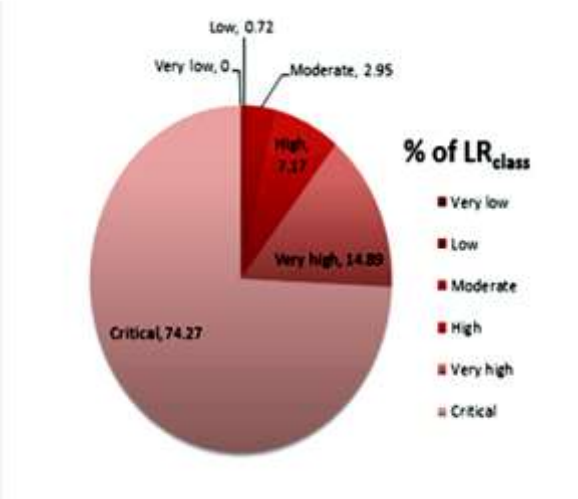

Figure 6a Percent of LRclass using FR model

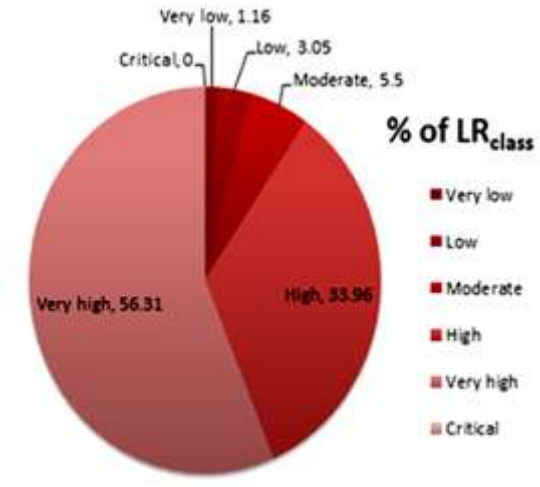

Figure 6b Percent of LRclass using Wi model

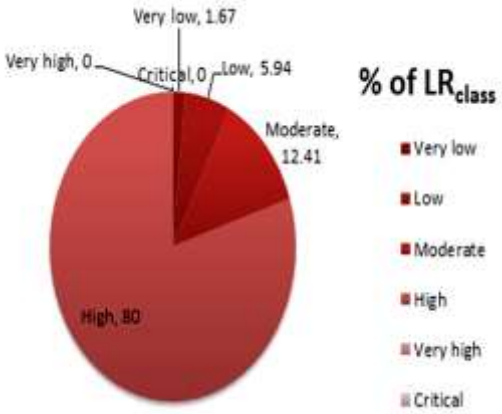

Figure 6c Percent of LR_{class} using Wf model

4.2 Receiver Operating Characteristics (ROC)

The receiver operating characteristics (ROC) is employed in this study to determine what areas might be affected by future landslides. A ROC curve is an effective way to indicate the quality of probabilistic and deterministic findings and forecast systems (Swets, 1988). In this study a ROC curve test was used as a cross-validation method. First, the historical landslide events were divided into two groups. The modeling group, which represented approximately 70% of the total landslides, was used as a training set to construct the susceptibility maps. The remaining 30% of landslides were used for prediction testing. The regions that were not affected by landslides were used as prediction group during the training phase. The regions affected by landslides were used in the training set labeled ‘‘areas prone to landslides.’’ The ROC curve was used to evaluate the prediction database and the region under the curve (AUC) was computed (Pradhan and Lee, 2010; Pradhan et al., 2010; Pourghasemi

et al., 2012). The AUC indicates how well a forecast system performed by determining how accurate the model was and if it was threshold independent (Yesilnacar and Topal, 2005). The result of sensitivity analysis indicated that the probabilistic frequency ratio model (Figure 7) was more efficient in terms of its predictions when compared to the other models used in this study.

The AUC for the landslide susceptibility map produced using the probabilistic frequency ratio model was 0.8154 (prediction accuracy = 81.5%) as determined by the ROC plot assessment. The AUC for the Wi and Wf models ranged from 0.7475 to 0.7305, respectively. With respect to predicted unstable pixels (Fig. 8), the AUC for the probabilistic frequency ratio was also the highest (0.7904), followed by the Wi model (0.7441), and the Wf model (0.7246) (Table 6). From the ROC curve test, it can be concluded that the probabilistic frequency ratio model was the best modeling technique used in this study.

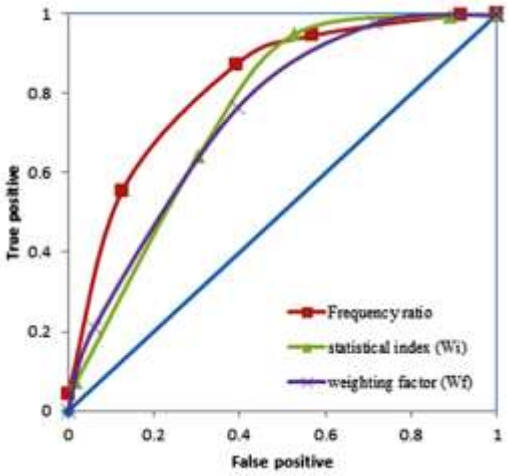

Figure 7 Success rate curves for the three landslide susceptibility maps

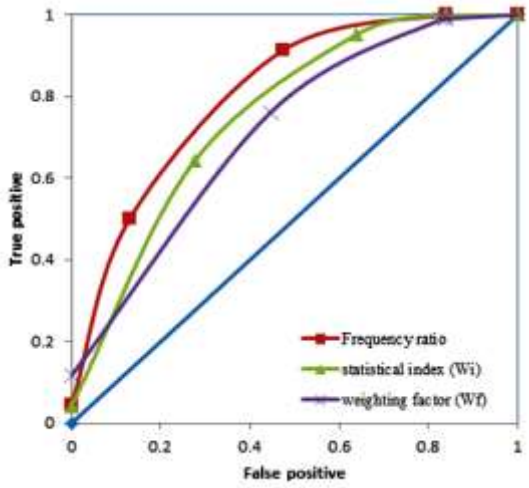

Figure 8 Prediction rate curves for the three landslide susceptibility maps

Table 6 Comparison of prediction rate curves for the three landslide susceptibility maps

Model	AUC	Prediction
Probability-Frequency ratio	0.7904	GOOD
Statistical index (Wi)	0.7441	GOOD
weighting factor (Wf)	0.7246	GOOD

5.0 CONCLUSION

This paper compared and evaluated three different models used to assess landslide susceptibility in the Hulu Kelang area of Kuala Lumpur, Malaysia. Three landslide susceptibility maps were produced and their reliabilities were verified by the receiver operating characteristics (ROC) of the susceptibility levels and active landslide zones.

LRclass is shown the predicted unstable area (Hazardous area ≥ High) has 96.37% chance of including the landslide using Fr model and have 90.27% and 80% chances using Wi, Wf models, respectively. Therefore, the landslide susceptibility map using the frequency ratio model preferred for use in this study as the resultant map contained a relatively low percentage of active landslide zones in the very low and low susceptibility classes, and a high percentage of active landslide zones in the high, very high and critical susceptibility zones.

The prediction rate of ROC curves for the susceptibility maps indicated that the probabilistic frequency ratio model had the highest prediction accuracy (>81%), while the Wf model showed the least prediction accuracy (73.05%). The verification results from the frequency ratio plots also indicated that the probabilistic frequency ratio method was a preferred landslide susceptibility assessment model for this area of study.

Acknowledgments

The authors acknowledge and appreciate the provisions of rainfall and landslide data by the Ampang Jaya Municipal Council (MPAJ), the Slope Engineering Branch of Public Works Department Malaysia (PWD), and the Department of Irrigation and Drainage Malaysia (DID), without which this study would not have been possible.

References

[1] Akgün, A, and F. Bulut. 2007. GIS-based landslide susceptibility for Arsin-Yomra (Trabzon, North Turkey) region. *Environmental Geology* 51: 1348–1377

[2] Ali, F. 2000. Unsaturated Tropical Residual Soils and Rainfall Induced Slopes in Malaysia. *Asian Conference on Unsaturated Soils Singapore*. 41(52): 18–19

[3] Carrara, A. 1983. A multivariate model for landslide hazard evaluation. Mathematical Geology 15: 403–426

[4] Cevik, E, and T. Topal. 2003. GIS-based landslide susceptibility mapping for a problematic segment of the natural gas pipeline, Hendek (Turkey). *Environmental Geology*. 44: 949–962

[5] Chung, C.J.F, and A.G. Fabbri. 2003. Validation of spatial prediction models for landslide hazard mapping. *Natural Hazards* 30: 451–472

[6] Conoscenti, C., D.M. Ciprioano, and E. Rotigliano. 2008. GIS analysis to assess landslide susceptibility in a fluvial basin of NW Sicily (Italy). *Geomorphology* 94: 325–339

[7] Dai, F.C., C.F. Lee, J. Li, and Z.W. Xu. 2001. Assessment of landslide susceptibility on the natural terrain of Lantau Island, Hong Kong. *Environmental Geology*. 43: 381–391

[8] Dahal, R.K., S. Hasegawa, A. Nonomura, M. Yamanaka, T. Masuda, and K. Nishino. 2008. GIS based weights-of-evidence modelling of rainfall-induced landslides in small catchments for landslide susceptibility mapping. *Environmental Geology*. 54: 311–324

[9] Dongyeob, K., I. Sangjun, H.L. Sang, H. Youngjoo, and C.H. Kyung-Sub. 2010. Predicting the rainfall-triggered landslides in a forested mountain region using TRIGRS model. *Journal of Mountain Science*. 7: 83–91

[10] Dwikorita, K., F.F. Teuku, I. Sudarno, A. Budi, L. Djoko, and W. B. Paul. 2011. Landslide hazard and community-based risk reduction effort in Karanganyar and the surrounding area, central Java, Indonesia. *Journal of Mountain Science.* 8: 149–153

[11] Ercanoglu, M., and C. Gokceoglu. 2002. Assessment of landslide susceptibility for a landslide-prone area (north of Yenice, NW Turkey) by fuzzy approach. *Environmental Geology* 41: 720–730

[12] Ercanoglu, M., C. Gokceoglu, and T.H.W.J. Van-Asch. 2004. Landslide susceptibility zoning north of Yenice (NW Turkey) by multivariate statistical techniques. *Natural Hazards* 32: 1–23

[13] Galli, M., F. Ardizzone, M. Cardinali, F. Guzzetti, and P. Reichenbach. 2008. Comparing landslide inventory maps. *Geomorphology* 94: 268–289

[14] García-Rodríguez, M.J., J.A. Malpica, B. Benito, and M. Díaz. 2008. Susceptibility assessment of earthquake-triggered landslides in El Salvador using logistic regression. *Geomorphology*. 95: 172–191

[15] Gruber, S.,and S. Peckham. 2008. Land-surface parameters and objects specific to hydrology. In Hengl T, Reuter HI, (eds.), Geomorphometry: *Concepts, Software and Applications. Developments in Soil Science*. 33:127–142

[16] Guzzetti, F., P. Reichenbach, M. Cardinali, M. Galli, and F. Ardizzone. 2005. Landslide hazard assessment in the Staffora basin, northern Italian Apennines. *Geomorphology*. 72: 272–299

[17] Guzzetti, F., P. Reichenbach, F. Ardizzone, M. Cardinali, and M. Galli. 2006. Estimating the quality of landslide susceptibility models. *Geomorphology*. 81: 166–184

[18] Kanungo, D.P., M.K. Arora, S. Sarkar, and R.P. Gupta. 2006. A comparative study of conventional, ANN black box, fuzzy and combined neural and fuzzy weighting procedures for landslide susceptibility zonation in Darjeeling Himalayas. *Engineering Geology*. 85: 347–366

[19] Lee, M.L., Y.N. Kim, F.H. Yuk, and C.L. Wei. 2013. Rainfall-induced landslides in Hulu Kelang area, Malaysia. Nat Hazards.

[20] Lee, S, and K. Min. 2001. Statistical analysis of landslide susceptibility at Yongin, Korea. *Environmental Geology*. 40: 1095–1113

[21] Lee, S. 2005. Application of logistic regression model and its validation for landslide susceptibility mapping using GIS and remote sensing data. *International Journal of Remote Sensing*. 26: 1477–1491

[22] Lee, S, and B. Pradhan. 2007. Landslide hazard mapping at Selangor, Malaysia using frequency ratio and logistic regression models. *Landslides*. 4: 33–41

[23] Lee, L.M., N. Gofar, and H. Rahardjo. 2009. A simple model for preliminary evaluation of rainfall-induced slope instability. *Geology Engineering*. 108(3–4): 272–285

[24] Mohammadi, M. 2008. *Mass movement hazard analysis and presentation of suitable regional model using GIS (Case Study: A part of Haraz Watershed).* M.Sc. Thesis. Tarbiat Modarres University International Campus, Iran

[25] Montgomery, D.R., W.E. Dietrich, R. Torres, S. P. Anderson, J.T. Heffner, and K. Loague. 1997. Hydrologic response of a steep, unchanneled valley to natural and applied rainfall. Water Recourse Research. 33: 91–109

[26] Mora, C.S, and W.G. Vahrson. 1994. Macrozonation methodology for landslide hazard determination. *Bulletin of the Association of Engineering Geologists*. 31: 49–58.

[27] Nandi, A, and A. Shakoor. 2009. A GIS-based landslide susceptibility evaluation using bivariate and multivariate statistical analyses. *Engineering Geology*. 110: 11–20

[28] Nefeslioglu,, H.A., T.Y. Duman, and S. Durmaz. 2008. Landslide susceptibility mapping for a part of tectonic Kelkit Valley (Easten Black Sea Region of Turkey). *Geomorphology*. 94: 401–418

[29] Nilsen, T.H., R.H. Wright, T.C. Vlasic, and W.E. Spangle. 1979. Relative slope stability and land-use planning in the San Francisco Bay Region, California, US. *Geological Survey Professional Paper*. 994: 96

[30] Oztekin, B, and T. Topal. 2005. GIS-based detachment susceptibility analyses of a cut slope in limestone, Ankara—Turkey. *Environmental Geology*. 49: 124–132

[31] Pourghasemi, H.R., B. Pradhan, C. Gokceoglu, M. Mohammadi, and H. R. Moradi. 2012. Application of weights-of-evidence and certainty factor models and their comparison in landslide susceptibility mapping at Haraz watershed, Iran. *Arabian Journal of Geosciences*. 14: 1–15

[32] Pradhan, B., R.P. Singh, and M. F. Buchroithner, 2006. Estimation of stress and its use in evaluation of landslide prone regions using remote sensing data. *Advances in Space Research*. 37: 698–709

[33] Pradhan, B, and S. Lee. 2010. Regional landslide susceptibility analysis using backpropagation neural network model at Cameron Highland, Malaysia. *Landslide*s. 7: 13–30

[34] Pradhan, B., S. Lee, and M.F. Buchroithner. 2010. Remote sensing and GIS based landslide susceptibility analysis and its cross-validation in three test areas using a frequency ratio model. Photogrammetrie Fernerkundung. *Geoinformation*. 1: 17–32

[35] Pradhan, B. 2012. A comparative study on the predictive ability of the decision tree, support vector machine and neuro-fuzzy models in landslide susceptibility mapping using GIS. *Computers & Geosciences*. 51: 350–365

[36] Refice, A, and D. Capolongo. 2002. Probabilistic modeling of uncertainties in earthquake induced landslide hazard assessment. *Computer Geoscience*. 28: 735–749

[37] Rutter, A.J., K.A. Kershaw, P.C. Robins, and A.J. Morton. 1971. A predictive model of rainfall interception in forests I. Derivation of the model from observations in a plantation of Corsican pine. *Agricultural and Forest Meteorology*. 9: 367–394

[38] Rutter, A.J., A.J. Morton, and P.C. Robins. 1975. A predictive model of rainfall interception in forests, II. Generalization of the model and comparison with observations in some coniferous and hardwood stands. *Journal of Applied Ecology*. 12: 367–380.

[39] Saadatkhah, N., A. Kassim, and L.M. Lee. 2014. Hulu Kelang, Malaysia regional mapping of rainfall-induced landslides using TRIGRS model. *Arabian Journal of Geosciences*. 1–12.

[40] Sarkar, S., D.P. Kanungo, A.K. Patra, and P. Kumar. 2008. GIS based spatial data analysis for landslide susceptibility mapping. *Journal of Mountain Science*. 5: 52–62

[41] Sarkar, S, and R. Anbalagan. 2008. Landslide hazard zonation mapping and comparative analysis of hazard zonation maps. *Journal of Mountain Science*. 5: 232–240
[42] Sidle, R.C., Y. Tsuboyama, S. Noguchi, I. Hosoda, M. Fujieda, and T. Shimizu. 2000. Stream flow generation in steep headwaters: a linked hydrogeomorphic paradigm. *Hydrological Process*. 14: 369–385
[43] Sidle, R.C, and M. Chigira. 2004. Landslides and debris flows strike Kyushu, Japan. *Transactions American Geophysical Union* 85(15): 145-151
[44] Sidle, R.C, and H. Ochiai. 2006. Landslides: Processes, Prediction, and Land Use. *Water Resource Monograph*. 18: 312
[45] Suzen, M.L, and V. Doyuran. 2004. Data driven bivariate landslide susceptibility assessment using geographical information systems: a method and application to Asarsuyu catchment, Turkey. Engineering Geology. 71: 303–321
[46] Swets, J.A. 1988. Measuring the accuracy of diagnostic systems. *Science*. 240: 1285–1293
[47] Thiery, Y., J.P. Malet, S. Sterlacchini, A. Puissant, and O. Maquaire. 2007. Landslide susceptibility assessment by bivariate methods at large scales: application to a complex mountainous environment. Geomorphology. 92: 38–59
[48] Tsukamoto, Y., T. Ohta, and H. *Noguchi. 1982. Hydrogeological And Geomorphological Studies Of Debris Slides On Forested Hillslopes In Japan.* IAHS Publication. 137: 89–98
[49] Uchida, T., K.I. Kosugi, and T. Mizuyama. 2002. Effects of pipe flow and bedrock groundwater on runoff generation in a steep headwater catchment in Ashiu, central Japan. *Water Resources Research* 38(111): 9–14
[50] Van-Westen, C.J. 1997. *Statistical Landslide Hazard Analysis, ILWIS 2.1 For Windows Application Guide*. ITC Publication Enschede. 73–84
[51] Wang, H.B, and K. Sassa. 2005. Comparative evaluation of landslide susceptibility in Minamata area, Japan. *Environmental Geology*. 47: 956–966
[52] Wilson, J.P, and J.C. Gallant. 2000. *Terrain Analysis Principles And Application*s. Wiley, New York, 303
[53] Yesilnacar, E, and T. Topal. 2005. Landslide susceptibility mapping: a comparison of logistic regression and neural networks methods in a medium scale study, Hendek region (Turkey). *Engineering Geology*. 79: 251–266
[54] Zhou, G., T. Esaki, Y. Mitani, M. Xie, and J. Mori. 2003. Spatial probabilistic modeling of slope failure using an integrated GIS Monte Carlo simulation approach. *Engineering Geology*. 68: 373–386